

High-spin structure of the neutron-rich $^{107,109}_{45}\text{Rh}$ isotopes: the role of triaxiality

Ts. Venkova¹, M.-G. Porquet², I. Deloncle², B.J.P. Gall³, H. De Witte², P. Petkov¹, A. Bauchet², T. Kutsarova¹, E. Gueorgieva⁴, J. Duprat⁵, C. Gautherin⁶, F. Hoellinger³, R. Lucas⁶, A. Minkova⁴, N. Schulz³, H. Sergolle⁵, E.A. Stefanova¹, A. Wilson^{2,a}

¹ INRNE, BAN, 1784 Sofia, Bulgaria

² CSNSM, IN2P3/CNRS and Université Paris-Sud, 91405 Orsay Campus, France

³ IReS, IN2P3/CNRS and Université Louis Pasteur, 67037 Strasbourg Cedex 2, France

⁴ University of Sofia, Faculty of Physics, 1126 Sofia, Bulgaria

⁵ IPN, IN2P3/CNRS and Université Paris-Sud, 91406 Orsay, France

⁶ DAPNIA/SPhN, CEA Saclay, 91191 Gif-sur-Yvette, France

Received: 1 September 1999

Communicated by D. Schwalm

Abstract. The $^{107,109}\text{Rh}$ nuclei have been produced as fission fragments following the fusion reaction $^{28}\text{Si} + ^{176}\text{Yb}$ at 145 MeV bombarding energy and studied with the Eurogam2 array. In both nuclei three new rotational bands with the odd proton occupying the $\pi g_{9/2}$, $\pi p_{1/2}$ and $\pi(g_{7/2}/d_{5/2})$ sub-shells have been observed. In ^{107}Rh , two other bands involving strong M1 transitions have been identified at excitation energy larger than 2 MeV. They can be interpreted in terms of three quasiparticle excitations. In addition new structures consisting of four transitions, built on states located at low excitation energy (680 keV in ^{107}Rh and 642 keV in ^{109}Rh), point out the importance of triaxial deformation in these two isotopes.

PACS. 21.60.Ev Collective models – 23.20.Lv Gamma transitions and level energies – 25.85.Ge Charged-particle-induced fission – 27.60.+j $90 \leq A \leq 149$

1 Introduction

The nuclides with $40 \leq Z \leq 50$ and $N \geq 50$ are of current interest because of the several shape transitions which occur in the $A \sim 100$ mass region. Different types of deformation (e.g. prolate, oblate, triaxial) are observed and can coexist in a same nucleus in accordance with the underlying interplay between orbitals. For $Z \geq 44$, the active intruder orbitals are near the top of the $\pi g_{9/2}$ subshell, this drives shapes towards oblate deformation. On the contrary, when the neutron Fermi level lies below or near the bottom of the $\nu h_{11/2}$ subshell (as for $N \sim 60$), the shape is driven to prolate deformation. In this region, the other neutron and proton states coming from the normal-parity subshells do not drive deformation very much, except the intruder $1/2^+[431]$ proton orbital originating from the $\pi(g_{7/2}/d_{5/2})$ sub-shells located above the $Z = 50$ major shell gap. This orbital is expected to have strong deforming effect towards well-elongated shapes. In fact the first members of the rotational band built on this intruder state have been observed at moderate excitation energies in nuclei near the $N = 66$ neutron mid-shell [1–4].

^a Present address: Dept. of Phys., Univ. of York, York Y01 5DD UK

Therefore these nuclei are good laboratories to study the influence of orbitals on deformation.

Previous to this work, the only information on the excited states of the neutron-rich $^{107,109}\text{Rh}$ isotopes was limited to spin values $I \leq 9/2$, since they are based on β -decay measurements [2,3] and particle transfer reactions [5]. The low-energy structures of the two isotopes look very similar. Their $7/2^+$ ground state and their first excited state $9/2^+$ come from the $\pi g_{9/2}$ subshell. Their first $5/2^-$ state decays by an E2 transition towards their $1/2^-$ isomeric state located at 268 keV in ^{107}Rh and 374 keV in ^{109}Rh . They are interpreted as first states of the $1/2^- [301]$ band from the $\pi p_{1/2}$ subshell. In addition the first members of the band corresponding to the intruder $1/2^+[431]$ state have been observed. Because of the value of the decoupling parameter, a ~ -1 , the sequence of rotational states is very peculiar, the $3/2^+$ level lies just below the $1/2^+$ band head, as well as the $7/2^+$ is located below the $5/2^+$ level [2,3].

The study of higher spin states of $^{107,109}_{45}\text{Rh}$ is very interesting in order to give a new insight on the shape of these two nuclei. Lying on the neutron-rich side of the stability line, the population of their high-spin levels via the usual (Heavy Ions, $xn\gamma$) fusion reactions is hindered by

the lack of suitable target-projectile combinations. Besides the so-called massive transfer or break-up fusion reactions, the spontaneous fission [6–8] and heavy-ion induced fission [9] have become the effective tool for such studies.

We report here results obtained in odd-A $^{103-109}\text{Rh}$ isotopes, populated as fragments of heavy-ion induced fission, focusing on new rotational bands observed in $^{107,109}\text{Rh}$ up to spin (29/2) and (25/2) respectively. Among them, four structures are very similar to the bands 1-4 already known in ^{103}Rh [10] and ^{105}Rh [11]. Moreover high-spin members of the rotational band built on the intruder orbital $1/2^+[431]$ is reported for the first time in an odd-A Rh isotopes. The nuclear shapes associated with all the rotational bands of ^{107}Rh are discussed in the framework of asymmetric rotor + quasiparticle model. This points out that (i) a triaxial deformation is inferred from the whole structure associated with the $\pi g_{9/2}$ sub-shell, (ii) the same nuclear shape can also account for the bands built on the $1/2^- [301]$ orbital from the $\pi p_{1/2}$ subshell and on the intruder $1/2^+[431]$ orbital from the $\pi(g_{7/2}/d_{5/2})$ sub-shells.

2 Experimental procedures and analysis

The $^{103-109}\text{Rh}$ isotopes have been produced as fission fragments of polonium isotopes obtained in the fusion reaction $^{28}\text{Si}+^{176}\text{Yb}$ reaction at 145 MeV beam energy. The beam was provided by the Vivitron accelerator at Strasbourg. A 1.5 mg/cm^2 target of ^{176}Yb was used, onto which a backing of 15 mg/cm^2 Au had been evaporated in order to stop the recoiling nuclei. The prompt γ -rays were detected with the Eurogam2 array [12], consisting of 54 escape-suppressed Ge detectors. Thirty of them were large-volume coaxial detectors positioned at backward and forward angles with respect to the beam axis. The remaining 24 detectors, arranged in two rings close to 90° to the beam direction, were four-element “clover” detectors. The data were recorded in an event-by-event mode with the requirement that a minimum of five unsuppressed Ge detectors fired in prompt coincidence. A total of 540 million coincidence events were collected, out of which 135 million were three-fold, 270 million four-fold and 108 million five-fold.

The off-line analysis consisted of both usual γ - γ sorting and multiple-gated spectra [13]. In addition, we analysed a three-dimensional “cube” built with the software of [14]. The latter technique was useful to make fast inspection of the data, which contain γ -ray cascades of more than 80 fission fragments as well as those of nuclei from the strong fusion-evaporation channels [15, 16].

The identification of transitions depopulating high-spin levels, which are completely unknown, such as those of $^{107,109}\text{Rh}$, is based on the fact that the prompt γ -rays emitted by complementary fragments are detected in coincidence [6, 9]. From our previous studies of other couples of complementary fragments observed in this experiment [16], we have deduced that the main complementary fragment of ^{107}Rh (^{109}Rh resp.) is ^{91}Y (^{89}Y resp.). Therefore

new transitions, depopulating high-spin states of ^{109}Rh for instance, can be identified from double gates set on one transition of ^{89}Y and one transition belonging to the low energy part of the ^{109}Rh level scheme, which is known from β -decay measurement, as reported above. Then these new transitions are used for further investigations of the coincidence data.

The problem of obtaining correct relative intensities, first exposed in ref [13], has been solved by creating multiple gated spectra directly from data on tapes with the code Fantastic [13]. In fission experiments, spin values can be assigned from angular correlation results [17]. The statistics of our present data was unfortunately too poor to perform such an analysis. Therefore, spin assignments are based upon (i) the already known spins of the band-head states [2, 3], (ii) the assumption that in yrast decays, spin values increase with the excitation energy, (iii) the analogy with the level structures of the less neutron-rich Rh isotopes, $^{103,105}\text{Rh}$ [10, 11].

3 Experimental results

Several Rh isotopes ($^{103-109}\text{Rh}$) are populated in the fusion-fission reaction used in this work, the maximum of the yields being centered around $A = 106$. Therefore the statistics is larger for $^{105,107}\text{Rh}$ as compared to the two other odd-A isotopes $^{103,109}\text{Rh}$. The high spin states of $^{103,105}\text{Rh}$, previously studied by means of heavy-ion induced reactions, are known up to spin (37/2) and (29/2) respectively [10, 11]. In this work, while we have observed the high-spin states of these two isotopes only up to spin (27/2), one new transition (461 keV) has been added at the top of band 4 of ^{105}Rh [11], populating the $25/2^-$ state at 3306 keV.

Examples of double-gated spectra showing new transitions depopulating high spin states of $^{107,109}\text{Rh}$ are shown in Figs. 1 and 2, respectively. The high-spin level scheme of ^{107}Rh , obtained in this work, is shown in Fig. 3. It has been obtained up to $I^\pi = (29/2^+)$ at an energy of 3801 keV. The yield of ^{109}Rh in our experiment is low, therefore its level scheme, shown in Fig. 4, is less developed as compared to the one of ^{107}Rh . The observed levels in $^{107,109}\text{Rh}$ are grouped into structures with rotational behaviours, labeled bands 1-7. Four of them are very similar to the bands 1-4 observed in ^{105}Rh [11] and in ^{103}Rh [10]. The band 5 of ^{107}Rh is built on the $3/2^+$ level assigned as the member of the $1/2^+[431]$ band, as mentioned above. This is the first time that the high spin part of this intruder band is observed in an odd-Rh isotope. On the other hand, while the 184 keV transition depopulating the $7/2^+$ member in ^{109}Rh has been clearly observed in our data, the higher spin states of the intruder band could not be identified.

Furthermore a new structure (labeled band 6) has been observed in both isotopes, built on states located at 680 keV in ^{107}Rh and 642 keV in ^{109}Rh , already known from radioactivity studies [2, 3]. This structure is mainly populated by the decay of band 7 in ^{109}Rh , which has no counterpart in ^{107}Rh , as discussed below.

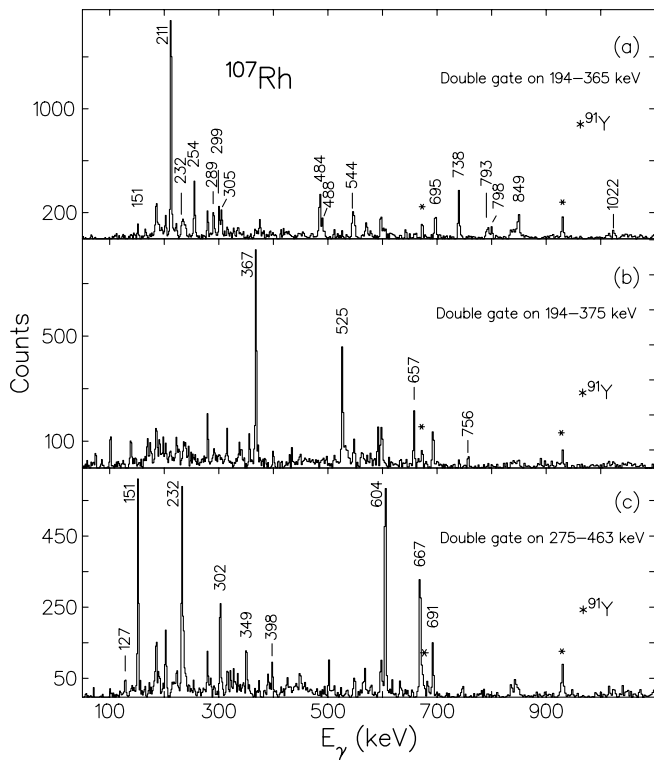


Fig. 1. Spectra of rays in double coincidence with two transitions of ^{107}Rh . The transitions marked with a star belong to the main complementary fragment, ^{91}Y

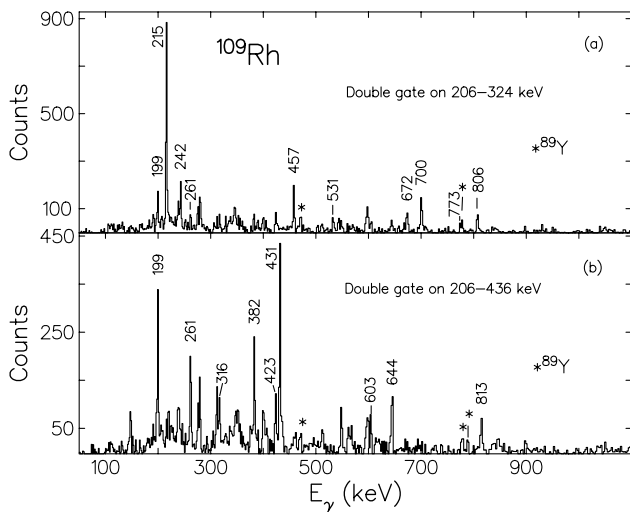


Fig. 2. Spectra of rays in double coincidence with two transitions of ^{109}Rh . The transitions marked with a star belong to the main complementary fragment, ^{89}Y

4 Discussion

4.1 Potential energy surfaces

Potential energy surfaces (PES) for the ground states of $^{105,107,109}\text{Rh}$ have been calculated in a microscopic self-consistent model including a delta type pairing treatment

by means of the Hartree-Fock + BCS + Lipkin-Nogami formalism, as described in refs [18]. The SLy4 interaction, constructed especially for the neutron-rich nuclei [19] has been used for the particle-hole channel.

The $^{105,107,109}\text{Rh}$ isotopes are odd-proton nuclei. Therefore one should use blocking procedure in order to get the right occupation number of the orbital located at the Fermi surface. The exploration of the complete (Q_t, γ) plane would imply to take into account the numerous changes of the configuration of the odd proton. In this work, we have chosen the same formalism as in even-even nuclei but with the additional requirement that the number of protons is odd, assuming that all the orbitals near the Fermi surface have a smooth behaviour with respect to Q_t and γ .

Figure 5 presents the PES obtained for the Rh isotopes and those for their neighbouring even-even cores, Ru and Pd. It displays the evolution of the shape of ground state of Rh isotopes as a function of mass number: the β deformation evolves from 0.20 to 0.26. The $^{106,108,110}\text{Pd}$ isotopes exhibit a prolate shape ($\gamma=0$) with a triaxial softness increasing with the number of neutrons. The $^{104,106,108}\text{Ru}$ nuclei are clearly triaxial with a γ parameter comprised between 16° and 30° . The $^{105,107,109}\text{Rh}$ isotopes show a shape transition: ^{105}Rh is predicted to be prolate as ^{106}Pd , and $^{107,109}\text{Rh}$ are expected to possess triaxial shapes as $^{106,108}\text{Ru}$.

4.2 $\pi g_{9/2}$ excitations and triaxial rotor + quasiparticle calculations

The excited states of ^{107}Rh have been calculated using the code Asyrmo which diagonalizes a particle + triaxial rotor Hamiltonian in the strong coupling basis, with the single particle matrix elements expressed in deformed scheme, as described in [20]. The single-particle energies and matrix elements are computed using a modified oscillator (Nilsson) potential. The parameters of the modified oscillator parameters, κ and μ , have been chosen according to ref [21], i.e. $\kappa_p = 0.069$ and $\mu_p = 0.45$ for $N=3$ and $N=4$ proton shells. As discussed below, the standard values of κ and μ [22] do not give good results for the location in energy of the natural-parity subshells, which would prevent the use of this model for the whole description of the bands built on all the proton sub-shells.

The values of the deformation parameters (ϵ, γ) have been extracted from the experimental properties of the ^{106}Ru core. The ratio of the energies of the two first 2^+ excited states gives the value of the γ parameter and the $B(E2; 2^+_1 \rightarrow 0^+)$ value determines the elongation parameter, once the γ parameter is known. Results, presented in Fig. 6, are in good agreement with the experimental levels coming from the $\pi g_{9/2}$ excitations (see Fig. 3). The signature splitting observed in the lowest structure is satisfactorily reproduced. Moreover another rotational band built on a second $11/2^+$ state is predicted below 800 keV and another structure built on an excited $3/2^+$ state is calculated below 600 keV: these two band heads come from

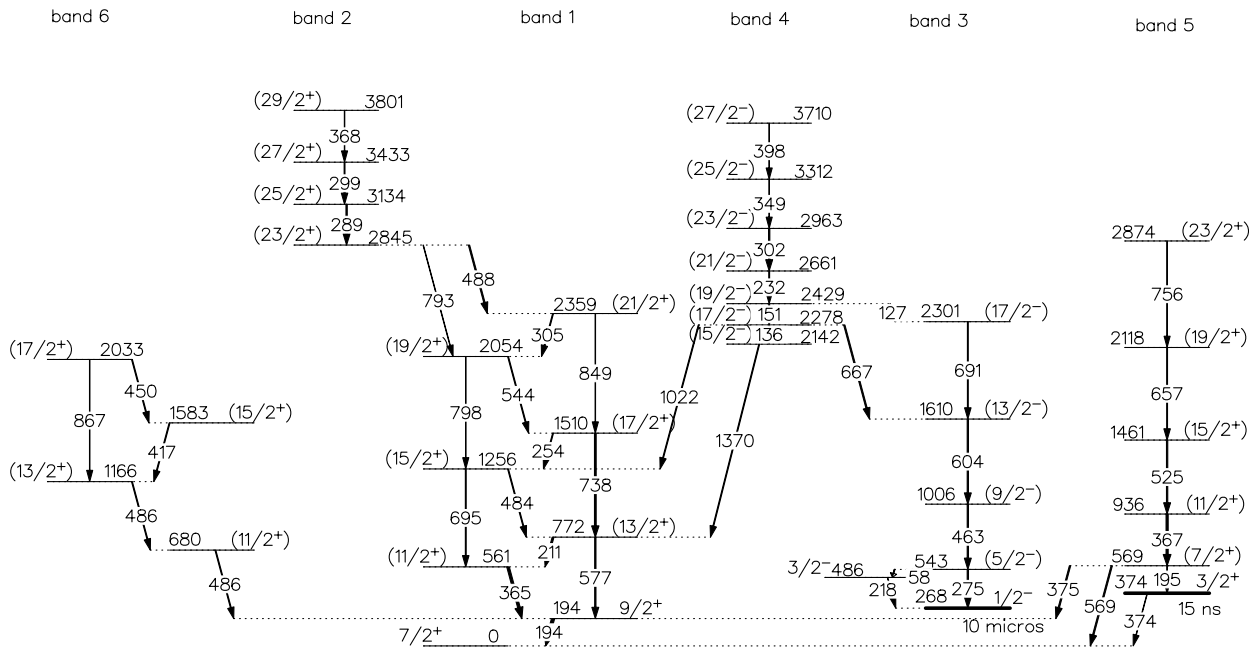


Fig. 3. High-spin level scheme of ^{107}Rh , obtained as a fission fragment in the fusion $^{28}\text{Si}+^{176}\text{Yb}$ reaction at 145 MeV beam energy. The spin and parity values of the excited states with spin values $\leq 9/2$ have been established from β -decay measurement [2]

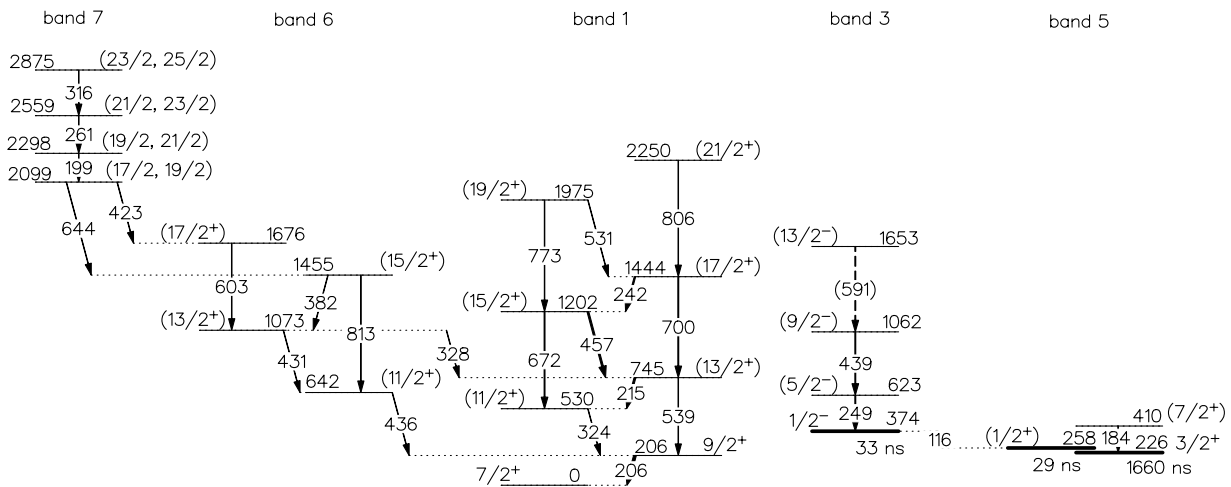


Fig. 4. High-spin level scheme of ^{109}Rh , obtained as a fission fragment in the fusion $^{28}\text{Si}+^{176}\text{Yb}$ reaction at 145 MeV beam energy. The spin and parity values of the excited states with spin values $\leq 9/2$ have been established from β -decay measurement [3]

the coupling of the $7/2^+[413]$ proton state¹ and the 2^+ γ -phonon of the core.

This can be respectively compared to our experimental band 6, observed in both isotopes (see Fig. 3 and Fig. 4),

¹ While large mixtures of different K states are expected in the triaxial region, the physical states obtained in this calculation involve mainly the $K=7/2^+[413]$ orbital from the $\pi g_{9/2}$ subshell

and to the $3/2^+$, $5/2^+$ states lying around 500 keV excitation energy and populated in the β -decay of odd-A Ru isotopes [2, 3]. Actually the existence of the second rotational structure is an evidence of the triaxiality of these Rh nuclei. The signature splitting, as observed in the main band built on the ground state, is also obtained for an axially-symmetric shape because of the large Coriolis coupling between the $5/2^+$ and $7/2^+$ states originating from the $\pi g_{9/2}$ subshell. Nevertheless for axially-symmetric shape,

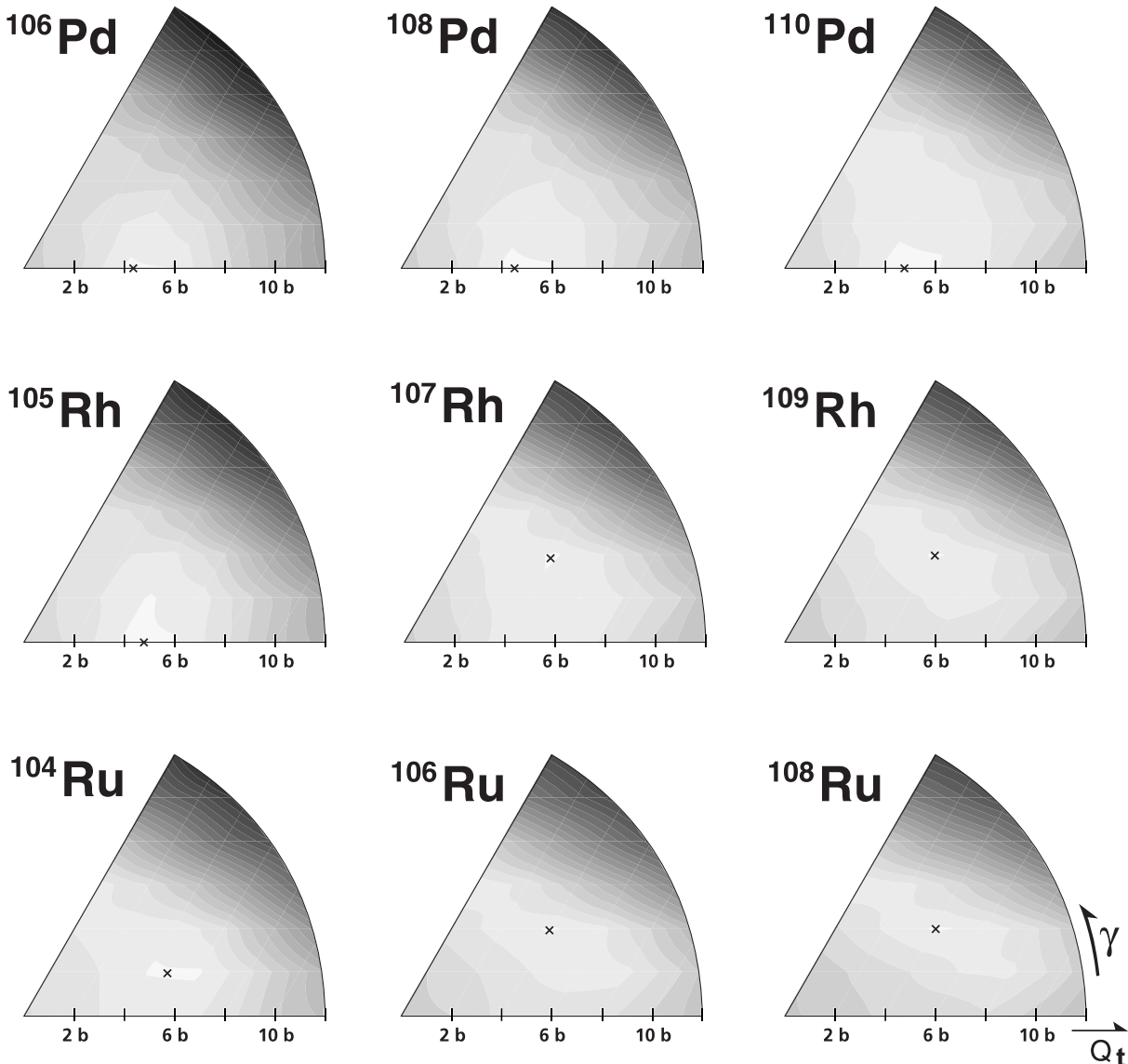


Fig. 5. Potential Energy Surface of $^{104,106,108}\text{Ru}$, $^{105,107,109}\text{Rh}$, and $^{106,108,110}\text{Pd}$, obtained via a Hartree-Fock + BCS + Lipkin-Nogami treatment. The first iso-energy is 70 keV above the minimum and the following ones are separated by 0.5 MeV. Q_t is the total (proton and neutron) quadrupole moment of the nucleus. The minima are indicated by a cross

the side band is completely different: another rotational band, built on the $5/2^+$ state is expected at very low excitation energy (Fig. 7).

4.3 Alignments and structure of three-quasiparticle bands

The alignments i (\hbar) for the bands 1, 2, 4 and 7 in $^{103-109}\text{Rh}$ are presented in Fig. 8 as a function of rotational frequency. They have been calculated following the procedure described in [23] with the Harris parameters, $\mathfrak{S}_0=8\hbar^2/\text{MeV}$, $\mathfrak{S}_1=25\hbar^4/\text{MeV}^3$, which have been obtained in such a way that the alignment plots of all calculated bands in these Rh isotopes exhibit flat behaviour after the first alignment. Around the frequency of 0.4 MeV, a band crossing is observed in band 1; above this crossing,

band 2 exhibits a gain in alignment of $8\hbar$ without signature splitting. These characteristics have been already interpreted for $^{103,105}\text{Rh}$ [10,11], in terms of $(\nu h_{11/2})^2$ pair breaking. The same conclusion holds for ^{107}Rh and the three-quasiparticle (3qp) configuration, $\pi g_{9/2} (\nu h_{11/2})^2$, is proposed to its band 2.

The increase of alignments between band 1 and band 4 observed in $^{103,105,107}\text{Rh}$ is around $5\hbar$. This value is very close to that obtained for the negative-parity bands of the neighbouring even-even nuclei (Ru, Pd). Moreover, the excitation energies of the corresponding band heads are very similar in the odd- Z and even-even nuclei, as shown in Fig. 9.

Therefore the configuration which can be assigned to band 4 involves a break of neutron pair, leading to a 3qp excitation, $\pi g_{9/2} \nu h_{11/2} \nu g_{7/2}/d_{5/2}$. It is worth noting that

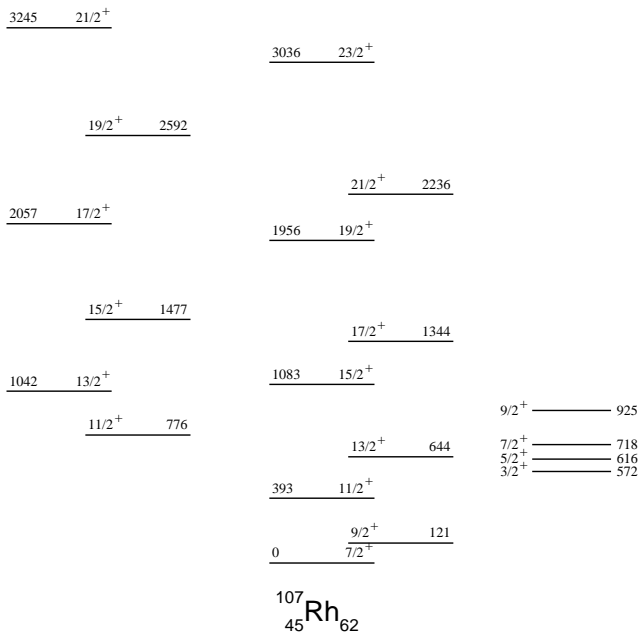


Fig. 6. Predictions of the asymmetric rotor model [20] for the $\pi g_{9/2}$ excitations in ^{107}Rh , obtained with the following parameters: $\epsilon=0.3$, $\gamma=23^\circ$, $E(2^+)=290$ keV

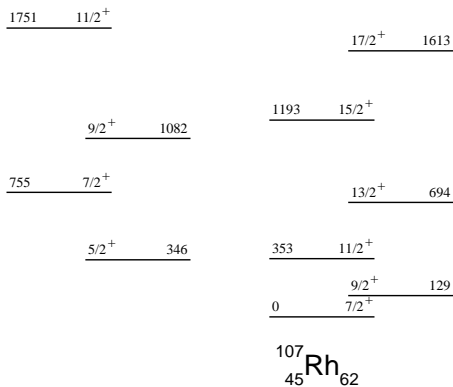


Fig. 7. Predictions of the asymmetric rotor model [20] for the $\pi g_{9/2}$ excitations in ^{107}Rh , obtained with the following parameters: $\epsilon=0.3$, $\gamma=0^\circ$, $E(2^+)=290$ keV

bands similar to this band 4 are known in several odd- Z nuclei in this mass region, ^{43}Tc , ^{45}Rh and ^{47}Ag , with $N \sim 60-64$.

The behaviour of band 7 of ^{109}Rh has to be underlined: the decay of its band head towards states belonging to the $\pi g_{9/2}$ excitation is neither comparable to this of band 2 nor to this of band 4 observed in $^{103,105,107}\text{Rh}$. Moreover the alignments computed for this band are very close to those obtained for band 4 of the lighter isotopes (see fig.8). The ^{109}Rh level scheme has to be extended in order to assign a configuration to this band 7, which is yrast in this energy range.

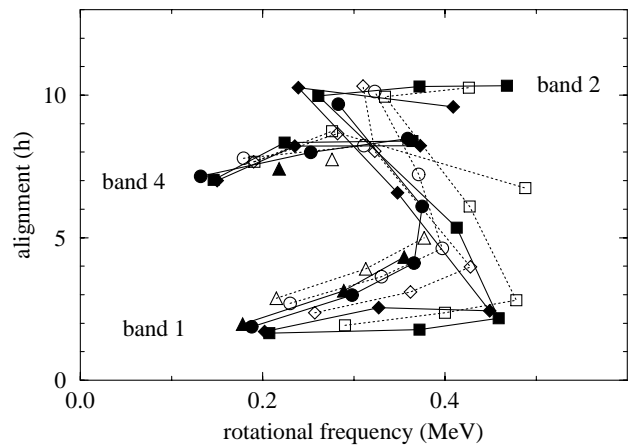


Fig. 8. Experimental alignments for bands 1, 2, 4 and 7 in ^{103}Rh (squares, [10]), ^{105}Rh (diamonds, [11] and this work), ^{107}Rh (circles, this work), ^{109}Rh (triangles up, this work). The filled symbols correspond to negative-signature states and the empty symbols to positive-signature states. The values of Harri parameters are $\mathfrak{I}_0=8 \hbar^2/\text{MeV}$, $\mathfrak{I}_1=25\hbar^4/\text{MeV}^3$

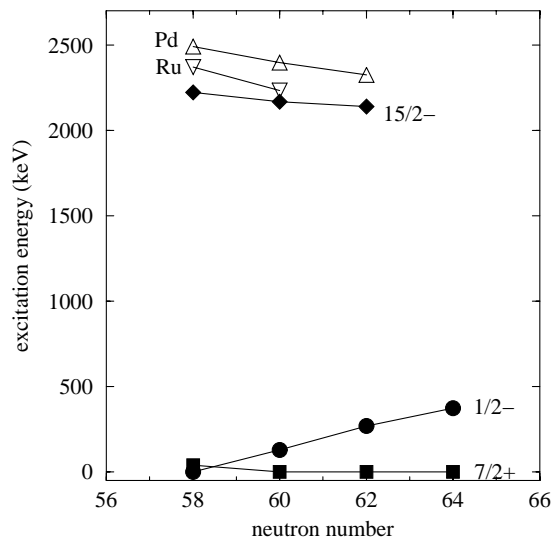


Fig. 9. Systematics of the excitation energies of the first 5^- state in even-even Ru (triangles down) and Pd (triangles up) nuclei with $N = 58-62$, as compared to the ones of the $15/2^-$ state observed in $^{103,105,107}\text{Rh}$ (filled diamonds). The ground state of ^{103}Rh is originating from $p_{1/2}$ subshell, while the ones of $^{105,107,109}\text{Rh}$ come from $g_{9/2}$ subshell

4.4 The intruder band $\pi 1/2^+[431]$

The intruder orbital $\pi 1/2^+[431]$ coming from the spherical $\pi(g_{7/2}/d_{5/2})$ sub-shells located just above the $Z = 50$ shell gap, appears at low excitation energy (below 400 keV for $^{107-109-111}\text{Rh}$) [1–4]. The main characteristic of the band built on this orbital is the value of the decoupling parameter, $a \sim -1$. So the $3/2^+$ level lies below the $1/2^+$ state. The $7/2^+$ and $5/2^+$ states, also identified from β -decay studies (see Fig. 4 of ref [1]), form the next doublet in energy. We have observed, for the first time, the

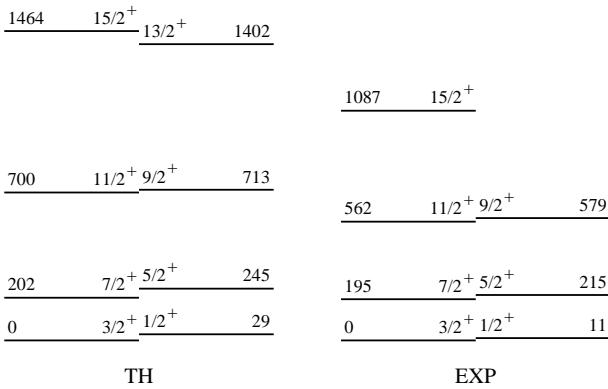


Fig. 10. Comparison of the low energy part of the experimental band 5 of ^{107}Rh (right; negative-signature states from this work; positive-signature states from [3]) and the predictions of the asymmetric rotor model (left), obtained for the band built on the intruder state $\pi 1/2^+$ [431], with the following parameters: $\epsilon=0.3$, $\gamma=23^\circ$, $E(2^+)=290$ keV

negative-signature part up to spin ($23/2^+$), in ^{107}Rh . Unfortunately, due to a lack of statistics, we have not been able to identify the high-spin part of this band in ^{109}Rh , although the decay of the $7/2^+$ state has been clearly observed in this work.

In a first attempt of describing the structure built on the intruder state, we have chosen the standard values [22] of the modified oscillator parameters, κ and μ , to obtain the single-particle energies and matrix elements needed for the code Asyrmo [20]. The resulting value of decoupling parameter was much larger than the experimental one (the $1/2^+$ state being close to $7/2^+$ one), whatever the values of deformation parameters, implying that the content of the wave function was wrong. New calculations have been done using other values of parameters, $\kappa_p = 0.069$ and $\mu_p = 0.45$ for $N=3$ and $N=4$ proton shells, as discussed in [21] and already used in this mass region [10] [24]. Figure 10 gives the comparison of experimental and calculated results. The band structure is basically well reproduced, except for the whole dilatation of the energy spectrum which is due to the rigid-rotor hypothesis.

It is worth noting that an upper limit for the lifetime of the very neutron deficient $^{81}_{41}\text{Tc}$ nucleus has been recently measured [25]. Microscopic-macroscopic calculations of its ground state predict that the equilibrium-deformation parameter is very large ($\beta \sim 0.44$) and the odd proton occupies the intruder $1/2^+$ [431] orbital [25]. Taking into account the value decoupling parameter of this orbital, one may expect that the spin value of the ground state of $^{81}_{41}\text{Tc}$ would be $3/2^+$, and not $1/2^+$.

4.5 The band $\pi 1/2^-$ [301]

Calculations with the code Asyrmo have been also performed for this structure (band 3), which is built on the $1/2^-$ [301] orbital from $\pi p_{1/2}$ sub-shell. Once more, the standard values of κ and μ [22] do not give satisfactory

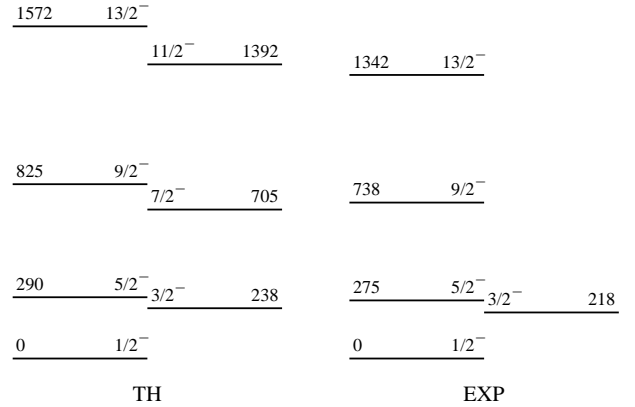


Fig. 11. Comparison of the experimental band 3 of ^{107}Rh (right) and the predictions of the asymmetric rotor model (left), obtained for the band built on the $1/2^-$ [301] state, with the following parameters: $\epsilon=0.3$, $\gamma=23^\circ$, $E(2^+)=290$ keV

results, as the $\pi f_{5/2}$ sub-shell is calculated too close to the $\pi p_{1/2}$ one. The comparison of experimental band 3 of ^{107}Rh with the theoretical results obtained with the other set of parameters is given in Fig. 11, the agreement is satisfactory.

In $^{105-107}\text{Rh}$, the decay of band 4 towards band 3 ($\pi p_{1/2}$ configuration) is very strong. This can be explained by the mixing of the two $17/2^-$ states of both configurations ($\pi p_{1/2}$ and $\pi g_{9/2} \nu h_{11/2} \nu g_{7/2} / d_{5/2}$) as they lie very close in energy. In some previous works, such a decay has been used to interpret the configuration of band 4 in terms of $\pi p_{1/2}$ configuration coupled to $\nu h_{11/2}^2$ or $\pi g_{9/2}^2$, while the excitation energy of band 4 seems too low for such a configuration.

4.6 Deformation of Rh and identical bands

Shape coexistence in odd-mass nuclei near closed shells (± 1 and ± 3 nucleons) has been reviewed some years ago [26]. For the odd-mass $_{49}\text{In}$ and $_{47}\text{Ag}$ nuclei, it has been shown that a $\pi g_{7/2} / d_{5/2}$ shell-model state intrudes across the $Z = 50$ shell closure giving rise to a rotational positive-parity band, coexisting with spherical states from $\pi(g_{9/2}, p_{1/2}, p_{3/2}, f_{5/2})$ subshells. Such a concept has been simply extended to the Rh ($Z = 45$) isotopes in order to interpret the main features of their low-spin states populated by the β -decay of odd-A Ru isotopes (see Fig. 4 of [1]).

The first fingerprint connected with shape coexistence in $_{45}\text{Rh}$ is the band-like structure built on the $1/2^+$ intruder state, while the lowest states remain interpreted in terms of spherical shape. The second fingerprint is related to the delayed electromagnetic transitions between the so-called coexisting states. The E2 transition connecting the lowest state of the intruder band, $3/2^+$, to the $7/2^+$ ground state is hindered, $F_W = 57$ in ^{109}Rh [3] and $F_W = 83$ in ^{111}Rh [1], compared to the Weisskopf single-particle estimates. The lower hindrance obtained in ^{107}Rh , $F_W = 6.6$ [2], can be explained in terms of mixing between the

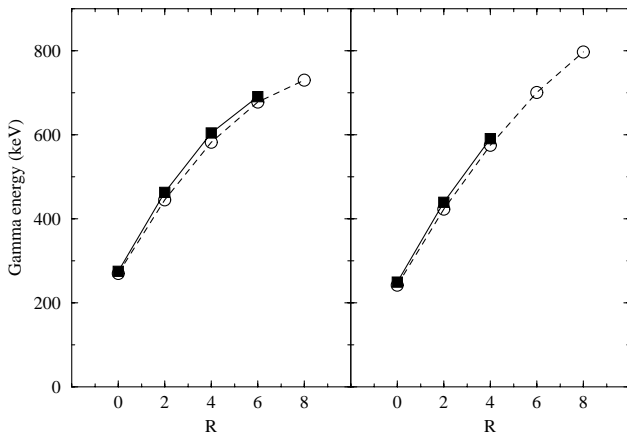


Fig. 12. Comparison of the γ -ray energies of band 3, $\pi 1/2^- [301]$ (filled squares), in ^{107}Rh (left) and ^{109}Rh (right) with those of corresponding cores (empty circles), the ground state bands in $^{106,108}\text{Ru}$ respectively. R is the rotational angular momentum of the core

$3/2^+$ state of the intruder band with another $3/2^+$ state located at 406 keV, from the $\pi g_{9/2}$ excitation.

The high-spin structures which have been identified in this work allow us to reconsider this interpretation, since the excited states coming from the $\pi g_{9/2}$ and $\pi p_{1/2}$ sub-shells correspond rather to deformed shape than spherical one, contrary to what observed in odd-mass ^{49}In and ^{47}Ag nuclei. As discussed above, the three rotational structures, built on $\pi g_{9/2}$, $\pi p_{1/2}$, and $\pi g_{7/2}/d_{5/2}$ sub-shells, can be correctly described within the framework of rigid-asymmetric-rotor + quasiparticle, using only one shape, with deformation parameters, $\epsilon=0.3$, $\gamma=23^\circ$. As for the hindered E2 transition decaying the $3/2^+$ state of the intruder band towards the $7/2^+$ ground state, it can be interpreted in terms of change of the K quantum number by three units ($K = 1/2$ towards $K = 7/2$), making it one-fold K -forbidden. Therefore its hindrance per degree of K forbiddenness would be $f_\nu = 57$ for ^{109}Rh and $f_\nu = 83$ for ^{111}Rh , which is typical for K -forbidden transitions [27].

It is worth noting that the $\pi 1/2^- [301]$ from the $p_{1/2}$ sub-shell is located near the Fermi surface for superdeformed (SD) nuclei with $Z = 64 - 66$. The occupation of this orbital led to the first observation of identical superdeformed bands [28]: the γ -ray sequences of an excited SD band of ^{151}Tb and the yrast SD band of ^{152}Dy have identical transition energies within one or two keV. This has been interpreted in term of the strong-coupling approach providing that the decoupling parameter value is $a = 1$ and that the occupation of the orbit does not modify the moment of inertia of the core [29]. A similar phenomenon occurs for $Z = 44 - 45$, as illustrated in Fig. 12 giving the comparison of the γ -ray energies of band 3 ($\pi 1/2^- [301]$) in $^{107,109}\text{Rh}$ with those of corresponding cores, the ground state bands in $^{106,108}\text{Ru}$ respectively. As expected for normally deformed nuclei, rotational bands remain identical over a smaller spin range than for SD nuclei.

5 Conclusion

The high efficiency of the γ -array Eurogam2 combined to an original use of a fusion-fission reaction mechanism is a very useful mean to reach high spin states of some neutron-rich nuclei, which cannot be populated otherwise. New band structures have been identified in $^{107,109}_{45}\text{Rh}$ isotopes, the odd proton occupying orbitals from the $\pi g_{9/2}$, $\pi p_{1/2}$ or $\pi (g_{7/2}/d_{5/2})$ sub-shells. The rotational bands are well described by using a triaxial-plus-particle model with the deformation parameter $\epsilon=0.3$, $\gamma=23^\circ$. The evidence of the deviation from the axial symmetry is given by the occurrence of side bands de-exciting towards the main $\pi g_{9/2}$ excitations. When approaching the $Z = 50$ closed shell, the collectivity is expected to be less and less marked. Studies of high spin states of ^{47}Ag and ^{49}In neutron-rich isotopes using the same approach are in progress.

The Eurogam project was funded jointly by IN2P3 (France) and the EPSRC (U.K.). We thank the crew of the Vivitron. We are very indebted to A. Meens for preparing the targets, G. Duchêne and D. Prévost for their help during the experiment. This work has been supported in part by the collaboration agreement Bulgarian Academy of Sciences-CNRS under contract No. 2937 and by the Bulgarian National Science Fund under contract No Ph565. The numerical calculations of the PES were carried out by the CRAY vector facilities of the IDRIS-CNRS center.

References

1. G. Lhersonneau et al., Eur. Phys. J. A. **1**, 285 (1998)
2. N. Kaffrel et al., Nucl. Phys. **A460**, 437 (1986)
3. N. Kaffrel et al., Nucl. Phys. **A470**, 141 (1987)
4. J. Rogowski, N. Kaffrel, D. De Frenne, K. Heyde, E. Jacobs, M.N. Harakeh, J.M. Schippers and S.Y. van der Werf, Phys. Lett. **B207**, 125 (1988)
5. J. Blachot, Nucl. Data Sheets **62**, 709 (1991) and **64**, 913 (1991)
6. M.A.C. Hotchkis et al., Nucl. Phys. **A530**, 111 (1991)
7. I. Ahmad and W.R. Phillips, Rep. Prog. Phys. **58**, 1415 (1995)
8. J.H. Hamilton, A.V. Ramayya, S.J. Zhu, G.M. Ter-Akopian, Yu. Ts. Oganessian, J.D. Cole, J.O. Rasmussen, and M.A. Stoyer, Prog. Part. Nucl. Phys. **35**, 635 (1995)
9. M.-G. Porquet et al., Workshop on the high angular momentum, Piaski, Poland (August 23-27, 1995), Acta Physica Polonica **27**, 179 (1996)
10. H. Dejbakhsh, R.P. Schmitt and G. Mouchaty, Phys. Rev. **C37**, 621 (1988)
11. F. R. Espinoza-Quiñones, E.W. Cybulska, J.R.B. Oliveira, M.N. Rao, M.A. Rizzutto, N.H. Medina, L.G.R. Emediato, W.A. Seale and S. Botelho, Phys. Rev. **C55**, 2787 (1997)
12. P.J. Nolan, F.A. Beck and D.B. Fossan, Ann. Rev. Nucl. Part. Sci. **44**, 561 (1994)
13. I. Deloncle, M.-G. Porquet, and M. Dziri-Marcé, Nucl. Instr. Meth. **A357**, 150 (1995)
14. D.C. Radford, Nucl. Instr. and Meth. **A361**, 296 (1995)

15. M.-G. Porquet et al., Proc. Int. Workshop on Research with Fission Fragments, Benediktbeuern, Germany, 28-30 Oct 1996, World Scientific, Singapore 1997, p. 149
16. M.-G. Porquet et al., International Symposium on Exotic Nuclear Shapes, Debrecen, Hungary (12-17 May 1997), APH N.S. Heavy Ions Physics **7**, 67 (1998)
17. W. Urban et al., Nucl. Inst. Meth. **A365**, 596 (1995)
18. B. Gall, P. Bonche, J. Dobaczewski, H. Flocard, and P.-H. Heenen Z. Phys. **A348**, 187 (1994) ; J. Terasaki, P.-H. Heenen, P. Bonche, J. Dobaczewski, and H. Flocard, Nucl. Phys. **A593**, 1 (1995) ; C. Rigollet, P. Bonche, H. Flocard and P.H. Heenen, Phys. Rev. **C59**, 3120 (1999)
19. E. Chabanat, P. Bonche, P. Haensel, J. Meyer, and R. Schaeffer, Nucl. Phys. **A627**, 710 (1997)
20. S. E. Larsson, G. Leander, and I. Ragnarsson, Nucl. Phys. **A307**, 189 (1978)
21. I. Ragnarsson and S.G. Nilsson, Proc. Colloquium on intermediate nuclei, Institut de Physique Nucléaire d'Orsay, 1971, p.112
22. T. Bengtsson and I. Ragnarsson, Nucl. Phys **A436**, 14 (1985)
23. R. Bengtsson and S. Frauendorf, Nucl. Phys. **A327**, 139 (1979)
24. W. Dietrich, A. Bäcklin, C.O. Lannergård and I. Ragnarsson, Nucl. Phys. **A253**, 429 (1975)
25. Z. Janas et al., Phys. Rev. Lett. **82**, 295 (1999)
26. K. Heyde, P. Van Isacker, M. Waroquier, J.L. Wood and R.A. Meyer, Phys. Rep. **102**, 292 (1983)
27. K.E.G. Löbner, Phys. Lett. **26B**, 369 (1968)
28. T. Byrski et al., Phys. Rev. Lett. **64**, 1650 (1990)
29. W. Nazarewicz, P.J. Twin, P. Fallon and J. D. Garrett, Phys. Rev. Lett. **64**, 1654 (1990)